Eur Biophys J (2011) 40:515–528
DOI 10.1007/s00249-011-0671-x

ORIGINAL PAPER

Cyclic antimicrobial R-, W-rich peptides: the role of peptide structure and *E. coli* outer and inner membranes in activity and the mode of action

Christof Junkes · Richard D. Harvey · Kenneth D. Bruce · Rudolf Dölling · Mojtaba Bagheri · Margitta Dathe

Received: 23 September 2010 / Revised: 7 December 2010 / Accepted: 3 January 2011 / Published online: 1 February 2011

Abstract This study compares the effect of cyclic R-, W-rich peptides with variations in amino acid sequences and sizes from 5 to 12 residues upon Gram negative and Gram positive bacteria as well as outer membrane-deficient and LPS mutant *Escherichia coli* (*E. coli*) strains to analyze the structural determinants of peptide activity. Cyclo-RRRWFW (c-WFW) was the most active and *E. coli*-selective sequence and bactericidal at the minimal inhibitory concentration (MIC). Removal of the outer membrane distinctly reduced peptide activity and the complete smooth LPS was required for maximal activity. c-WFW efficiently permeabilised the outer membrane of *E. coli* and promoted outer membrane substrate transport. Isothermal titration calorimetric studies with lipid A-, rough-LPS (r-LPS)- and smooth-LPS (s-LPS)-doped POPC liposomes demonstrated the decisive role of O-antigen and outer core polysaccharides for peptide binding and partitioning. Peptide activity against the inner *E. coli* membrane (IM) was very low. Even at a peptide to lipid ratio of 8/1, c-WFW was not able to permeabilise a phosphatidylglycerol/phosphatidylethanolamine (POPG/POPE) bilayer. Low influx of propidium iodide (PI) into bacteria confirmed a low permeabilising ability of c-WFW against PE-rich membranes at the MIC. Whilst the peptide effect upon eukaryotic cells correlated with the amphipathicity and permeabilisation of neutral phosphatidylcholine bilayers, suggesting a membrane disturbing mode of action, membrane permeabilisation does not seem to be the dominating antimicrobial mechanism of c-WFW. Peptide interactions with the LPS sugar moieties certainly modulate the transport across the outer membrane and are the basis of the *E. coli* selectivity of this type of peptides.

Keywords Antimicrobial · Cyclic peptides · Membrane permeabilisation · Uptake · Lipopolysaccharides

Introduction

A great deal of interest has been focused on antimicrobial peptides (AMPs) as a potential alternative class of antimicrobial agents because of their selectivity for prokaryotic cells and promise of minimizing the development of bacterial resistance (Hancock and Sahl 2006). Both of these attributes are facilitated by their mode of action, since most of the AMPs known so far are thought to act by permeabilisation of target cell membranes. Because of their cationic charge, the peptides accumulate at the negatively charged membrane of bacteria and their amphipathic nature allows partitioning into the lipid matrix, with subsequent pore formation resulting in cell death.

Among the structurally diverse AMPs, small sequences rich in particular residues such as tryptophan (W) and arginine (R) are of particular interest (Chan et al. 2006). Mostly, they represent antimicrobial motifs in larger

Membrane-active peptides: 455th WE-Heraeus-Seminar and AMP 2010 Workshop.

C. Junkes · M. Bagheri · M. Dathe (✉)
Leibniz Institute of Molecular Pharmacology (FMP), Robert-Roessle-Str. 10, 13125 Berlin, Germany
e-mail: dathe@fmp-berlin.de

R. D. Harvey · K. D. Bruce
Institute of Pharmaceutical Science, King's College London, 150 Stamford Street, London SE1 9NH, UK

R. Dölling
Biosyntan GmbH, Robert-Roessle-Str. 10, 13125 Berlin, Germany

natural proteins and because of their small size they are considered to be strong candidates for the development of new antibiotics by peptide engineering (Hilpert et al. 2005; Park et al. 2008). Recent studies have shown that cyclisation of a linear R-, W-rich hexapeptide and arrangement of the three aromatic residues in an aromatic cluster particularly enhanced the peptide activity against *E. coli* (Appelt et al. 2005; Dathe et al. 2004; Wessolowski et al. 2004). This apparent specificity has been suggested to depend upon the amino acid arrangement in the cycles. Either hydrophobic interactions with the fatty acid chains of lipid A or charge interactions disturbing the polar core polysaccharide region of the lipopolysaccharides (LPS) predominate in the disruption of the barrier function of the outer membrane. According to the current model of linear AMP activity, this breach of the outer membrane theoretically leads to exposure of the target plasma membrane to peptide action. However, recent studies on membrane permeabilisation and on the kinetics of cell death have also led to speculation of the involvement of other mechanisms in growth inhibition and killing of bacteria by small cyclic peptides (Junkes et al. 2008).

In this study we have compared the activity of a novel series of cyclic R-, W-rich peptides upon intact bacteria, outer membrane (OM)-deficient strains and LPS mutant strains of *E. coli*, and eukaryotic cells. For each of the peptides, the secondary structural properties were first characterised using circular dichroism (CD)-spectroscopy. We then investigated the permeabilising effect of the most active peptide upon both inner and outer *E. coli* membranes and analyzed the permeabilisation of lipid bilayers mimicking the properties of different putative target membranes. Peptide binding to LPS-doped bilayers was determined using fluorescence spectroscopy and isothermal titration calorimetry (ITC), to get insight into the driving forces of the interaction with the different cellular membranes. The results provide insight into the activity-relevant structural motifs of the peptides, facilitated identification of the membrane components which influence the mechanism of action, and allowed us to elucidate the role of LPS in the *E. coli* selectivity of cyclic hexapeptides.

Materials and methods

Materials

Chemicals for peptide synthesis and characterization were as follows: acetonitrile (J. T. Baker, Germany), Cerium(IV) ammonium nitrate (CAN), dichloromethane (DCM; Roth, Germany), N,N′-diisopropylethylamine (DIEA; Biosolve, Netherlands), N,N-dimethylformamide (DMF; Biosolve, Netherlands), N-[(dimethylamino)-1H-1,2,3-triazolo[4,5-b] pyridine-1-yl-methylene]-N-methylmethanaminium hexafluorophosphate N-oxide (HATU; GL Biochem, China), hexafluoroisopropanol (HFIP; ACROS, Belgium), 1,2,3-N-Hydroxybenzotriazole-1-ol (HOBt; IRIS, Germanys, 2-(1H-Benzotrialzole-1-yl)-1,1,3,3-tetramethyluronium tetrafluoroborate (TBTU; IRIS, Germany), trifluoroacetic acid (TFA; Fluka, Germany). The protected amino acids were from IRIS, Germany.

Other chemicals used were: calcein (Fluka, Germany), guanidine hydrochloride (GuHCl; Sigma–Aldrich, Germany), (3-(4,5-dimethyl-thiazol-2-yl)-2,5-diphenyl) tetrazolium bromide (MTT; Sigma–Aldrich, Germany), nitrocefin (NCF; Oxoid, UK), O-nitrophenyl-β-galactoside (ONPG; Sigma–Aldrich, Germany), polymyxin B sulphate (PMX; Fluka, Germany), propidium iodide (PI; Appli-Chem, Germany), tris(hydroxymethyl)aminomethane (Tris; Merck, Germany), Triton X-100 (Merck, Germany), trifluoroethanol (TFE; Riedel-de Haen, Germany). Other laboratory chemicals used for buffer preparation or as solution additives were purchased from Fluka, Germany.

The lipids, 1-palmitoyl-2-oleoyl-*sn*-glycero-3-phosphocholine (POPC), 1-palmitoyl-2-oleoyl-*sn*-glycero-3-[phospho-rac-(1-glycerol) (POPG) and 1-palmitoyl-2-oleoyl-*sn*-glycero-3-phospho-ethanoleamine (POPE) were provided by Avanti Polar Lipids, USA.

Cholesterol (Chol), lipid A (LA) from *E. coli* F583, rough lipopolysaccharide (r-LPS; Rd-LPS from *E. coli* F-583) and smooth LPS (s-LPS; from *E. coli* K-235) were purchased from Sigma–Aldrich, Germany.

In cell experiments the following media were used: lysogeny broth (LB; Sigma–Aldrich, Germany), LB Agar (Sigma–Aldrich, Germany), Mueller–Hinton Broth (Becton–Dickinson, Germany), Brain Heart Infusion Broth (BHI; Becton–Dickinson, Germany), Dulbecco's modified Eagle Medium (DMEM; Biochrom, Germany) and Phosphate buffered saline (PBS; Biochrom, Germany).

The following bacterial strains and cell lines were used: *Bacillus subtilis* (*B. subtilis*) (DSM357) and *E. coli* (DH5α) and (ML-35p) (Lehrer et al. 1988) strains, L-form *E. coli* W*1655 F+* cells (LWF+) and *B. subtilis* (L170) (Schuhmann and Taubeneck 1969), LPS carbohydrate mutant strains (CGSC, The Coli Genetic Stock Center, Yale University, New Haven, USA) D21 (rfa+), D21e19 (rfa-11), D21e7 (rfa-1), D21f1 (rfa-1, rfa-21), D21f2 (rfa-1, rfa-31) (Eriksson-Grennberg et al. 1971), HeLa cells (human cervix carcinoma), and human red blood cells (RBCs; Charité, Universitätsmedizin-Berlin, Germany).

Peptides

The cyclic peptides (Table 1) were prepared by multiple peptide synthesis (Schnorrenberg and Gerhardt 1989) on a SYRO synthesizer (MultiSynTec, Germany) using the

Table 1 Peptide characteristics

Abbreviation	Peptide sequence	t_R (min)	MIC (μM)		MIC (μM) L-form		Hemoglobin release (%) at 100 μM	Toxicity HeLa (%) at 100 μM
			E. coli DH5α	*B. subtilis* DSM357	*E. coli* L-WF+	*B. subtilis* L-170		
c-WFW	cyclo-(RRRWFW)	19.9	4	3	18	50	7	2
c-FFF	cyclo-(RRRFFF)	18.3	56	16	38	>100	3	10
c-WWW	cyclo-(RRRWWW)	20.2	11	3	19	50	6	14
c-www	cyclo-(rrrwww)	20.2	9	3	25	50	8	13
c-WRW	cyclo-(RWRWRW)	17.0	23	9	50	>100	2	1
c-wrw	cyclo-(rwrwrw)	17.0	21	9	50	>100	2	13
c-WFW5	cyclo-(RRWFW)	22.3	8	4	10	38	10	0
c-WFW8a	cyclo-(RRRRWFWF)	21.3	6	3	6	21	9	16
c-WFW10a	cyclo-(RRRRRWFWFW)	22.4	5	3	6	25	31	94
c-WFW12	cyclo-(RRRRRRWFWFWF)	23.5	4	1.5	6	6	58	97
KLA1	KLALKLALKAWKLALKAA-NH_2	20.4	5.2	1.6	10	1.6	100	ND

Lowercase letters refer to D-amino acid residues. t_R denotes the retention time in reversed phase high-performance liquid chromatography. MIC values give the minimal inhibitory concentration of growth of *E. c.* and *B. s.* as well as *E. c.*-derived L-form L-WF+ and outer wall-deficient *B. s.* L170. The hemolytic activity against human red blood cells was determined at 100 μM peptide concentration. The cytotoxic peptide effect towards HeLa cells was determined after 30 min of incubation using the MTT-viability assay. The mean MICs were obtained from at least three independent experiments performed in duplicate. Data for KLA1 have been partially published before (Dathe et al. 2002). *ND* not determined

(9-fluorenylmethoxycarbonyl) Fmoc/But strategy according to SHEPPARD (Chan and White 2000). Cleavage of the linear protected peptides from resin, cyclisation and removal of protecting groups were all performed according to established procedures (Chan and White 2000; Pearson et al. 1989; Deres et al. 1989). Analytical and preparative high performance liquid chromatography (HPLC) were performed using a Shimadzu LC-9A system equipped with a photodiode array detector SPD-M6A, column: Ultrasep ES (RP-18) 7 μm (250 × 3.0 mm) (SEPSERV GmbH, Germany) and a Shimadzu LC-8A systems with a UV–Vis-detector SPD-6A, column: Ultrasep ES (RP-18) 10 μm (250 × 20 mm) (SEPSERV GmbH, Germany), respectively, both operating at 220 nm. The mobile phase A was 0.05% TFA in water, phase B was 0.05% TFA in 80% ACN in water. A flow of 0.6 ml/min and linear gradient of 2.5% phase B/min were used. KLA1 (KLAL KLAL KAW KAAL KLA-NH_2) was synthesized by automated solid-phase synthesis and characterized as described previously (Dathe et al. 1996). Counterions were replaced with chloride by repeated lyophilisation of the peptides dissolved in 0.01 N HCl. The purity of the final products was >95% by analytical HPLC, and their expected molar mass was confirmed by matrix-assisted laser desorption/ionization time-of-flight mass spectrometry (MALDI-TOF) performed on a MALDI 2 instrument (Shimadzu Kratos, Japan).

HPLC

The HPLC retention time (t_R) of the peptides was determined on a Jasco HPLC system (Japan) as previously described, (Dathe et al. 2004) using a diode array detector operating at 220 nm. The sample concentration was 1 mg/ml peptide in eluent A. The mobile phase A was 0.1% TFA in water, and B was 0.1% TFA in 80% acetonitrile, and 20% water (v/v). The t_R was determined using a linear gradient of 5–95% B over 40 min at room temperature.

Liposome preparation

Stock solutions of POPC, POPG, POPE, Chol, lipid A, r-LPS or s-LPS dissolved in chloroform were used to produce the desired mixtures and molar lipid ratios at final concentrations between 5 and 20 mM. After drying, the lipid films were suspended in the desired buffer by vortexing. Small unilamellar vesicles (SUVs) for CD spectroscopic and W-fluorescence spectroscopic studies were prepared in buffer (10 mM NaH_2PO_4/Na_2HPO_4, 154 mM NaF, pH 7.4) by sonication using a Labsonic L ultrasonicator (B. Braun Biotech, Germany) as previously described (Dathe et al. 2004). Large unilamellar vesicles (LUVs) containing dye (70 mM calcein, 10 mM Tris, 0.1 mM EDTA, pH 7.4) were prepared by 35 fold extrusion across two stacked filters (100 nm pore size) using a mini extruder (Avestin, Switzerland). For vesicle aggregation studies, LUVs of different lipid compositions were prepared in 10 mM Tris, 154 mM NaCl, pH 7.4. For isothermal titration calorimetric (ITC) studies, SUVs composed of POPC and lipid A, r-LPS or s-LPS at a molar ratio of 12/1 were prepared in phosphate buffer (10 mM NaH_2PO_4/Na_2HPO_4, 154 mM NaF, pH 7.4) as described previously (Bagheri et al. 2011).

CD spectroscopy

CD spectra of the peptides were measured between 260 and 200 nm on a Jasco 720 spectrometer (Japan) as previously described, (Dathe et al. 2004) using phosphate buffer (10 mM NaH_2PO_4/Na_2HPO_4, 154 mM NaF, pH 7.4) and in the presence of 10 mM POPG-SUVs. Measurements in the near UV between 340 and 250 nm were performed in buffer at 20 and 80°C and in the presence of 50% (v/v) TFE or 4 mM GuHCl. The peptide concentration was 100 μM for measurements in a 2 mm pathlength cell (far UV) and a 5 mm pathlength cell (near UV range). The results are presented as mean residue ellipticities, Θ_{mr}.

Peptide fluorescence

Peptide binding to SUVs was followed by detecting changes in the tryptophan fluorescence monitored between 300 and 420 nm (excitation at 280 nm) on a Jasco FP-6500 spectrofluorimeter (Japan) (Dathe et al. 2004). The concentration of peptides in buffer (10 mM NaH_2PO_4/Na_2HPO_4, 154 mM NaF, pH 7.4) was 5 μM, the total lipid concentration of the POPC and POPC/POPG SUV suspensions used, was 1 mM.

Dye release

Peptide-induced calcein release was monitored fluorimetrically by measuring the time-dependent decrease in dye self-quenching (excitation at 490 nm, emission at 514 nm) at room temperature on an LS 50B spectrofluorimeter (Perkin Elmer, Germany) as described in an earlier paper (Dathe et al. 2004). The lipid concentration was 24 μM in Tris buffer (10 mM Tris, 154 mM NaCl, pH 7.4), the peptide concentrations ranged between 1 and 200 μM. The release data presented were obtained after 1 min of incubation.

Vesicle aggregation

Peptide-induced increase of vesicle size was monitored by dynamic light scattering (N4 Plus, Beckman Coulter, Germany) of LUVs containing lipids at different molar ratios (POPC/Chol 3/1, POPE/POPG 1/3, POPE/POPG 3/1, POPC/POPG 1/3, POPC/POPG 3/1) alone, in the presence of 10 μM c-WFW, and in the presence of peptide with 0.4% Triton X-100. The lipid concentration in each case was 24 μM.

The time course of the change in the LUV particle size was followed by measuring the optical density (OD) at 400 nm on a V-550 spectrometer (Jasco, Japan). To LUVs at a lipid concentration of 20 μM, aliquots of a c-WFW solution were added to change the peptide concentration in the measuring cell in 1 or 25 μM steps. Without stirring the suspension, changes in OD were followed for several hours. After reaching constant high OD values, the stirrer was switched on and after the OD had returned to its initial low values, the stirrer was switched off again and the absorption was followed over another 40–60 min.

Titration calorimetry

High-sensitivity ITC was performed on a VP-ITC (GE Healthcare, Sweden) at 37°C as previously described (Bagheri et al. 2011; Dathe et al. 2004). In a typical experiment, a 40 μM peptide solution in the calorimeter cell was titrated with 3–10 μL of SUV suspension with lipid concentrations of 5 mM (s-LPS/POPC 1/12 mol/mol) and 20 mM (r-LPS/POPC 1/12 mol/mol, lipid A/POPC 1/12 mol/mol). The cumulative heat of reaction as a function of the number of injections was used to derive binding isotherms. To evaluate the data, the surface partitioning model was used in combination with the Gouy–Chapman theory (to consider electrostatic interactions), both of which are explained in detail elsewhere (Keller et al. 2006; Seelig 1997). The molar ratio of bound peptide over accessible lipid, R_b, is defined as $R_b = c_{p,b}/\gamma\, c_L$ where $c_{p,b}$ denotes the concentration of peptide bound to bilayer membranes and c_L the total lipid concentration. γ is the lipid accessibility factor (0.6 for membrane-impermeant peptides interacting with SUVs). On the basis of the model, we fitted the ITC data to obtain the partition coefficient, K_0 and the molar enthalpy of membrane partitioning, $\Delta H°$. The Gibbs free energy of membrane partitioning, $\Delta G°$ was then taken as $\Delta G° = -RT \ln 55.5\ K_0$.

Antimicrobial activity

The minimal inhibitory concentration (MIC) of bacterial growth was determined using a microdilution assay as previously described (Junkes et al. 2008; Wiegand et al. 2008). The peptide activity was tested against Gram positive *B. subtilis* (DSM357) and Gram negative *E. coli* (DH5α and ML-35p) cultivated in LB. The inoculum was prepared from mid log phase cultures ($OD_{625} = 0.4 \pm 0.1$), to give a final number of cells per well of 5×10^5. The final concentrations of peptides ranged from 0.1 to 200 μM. L-form *E. coli* W*1655 F+* cells (LWF+) and *B. subtilis* (L170) were cultivated in BHI medium containing 0.6 mg/ml penicillin, and for L170 additionally 30 mg/ml sucrose and 10 mg/ml yeast extract. The L-form bacteria were grown until OD_{625} of 0.8 and then diluted to 0.4. 20 μl of the cell suspension was added to 180 μl peptide solution to reach a final peptide concentration between 0.05 and 100 μM. The peptides were tested in duplicate in at least three independent experiments. After

incubating the plates overnight at 37°C whilst shaking at 180 rpm, the absorbance was measured at 600 nm (Safire Microplate Reader, Tecan, Germany). The MIC is defined as the lowest concentration of peptide for which no change in optical density could be observed.

Activity towards LPS carbohydrate mutant strains

The peptides were assayed against wild type and rough mutant strains of *E. coli* expressing different LPS chemotypes, as described elsewhere (Farnaud et al. 2004; Junkes et al. 2008). The strains can be grouped according to the affected region of their LPS. The relevant genotype of the K12 strains is as follows: D21 (rfa+), D21e19 (rfa-11), D21e7 (rfa-1), D21f1 (rfa-1, rfa-21), D21f2 (rfa-1, rfa-31). The bacteria were cultured in LB at 37°C and MICs were obtained using the classical microtiter broth dilution assay. The final number of cells per well was 5×10^5, and the final concentrations of peptides, tested in duplicate, ranged from 0.05 to 100 μM. The mean MICs presented were obtained from 5 independent experiments, each performed in duplicate.

Bacterial killing assay

The assay was performed with LPS-mutant strains as recently described elsewhere (Friedrich et al. 2000; Junkes et al. 2008). The setup and the co-incubation of bacteria with peptides was the same as described above for the antimicrobial activity test. At time intervals of 1, 10, 30, 60 and 120 min, samples were removed, diluted 50-fold (peptide-treated) or 5,000-fold (untreated control), and 50 μl samples of the dilution were plated onto agar plates. After overnight incubation at 37°C the colonies (CFUs) were counted.

Inner and outer membrane permeabilisation

The membrane permeabilising activity of peptides was assessed against *E. coli* (ML-35p) in 96-well microtiter plates as previously described (Junkes et al. 2008; Lehrer et al. 1988). The wells contained the peptide at various concentrations in LB, cells at an optical density OD_{600} of 0.1 (corresponding to 10^7 cells/ml), and 20 μg/ml NCF or 100 μg/ml ONPG to monitor outer and inner membrane permeabilisation, respectively. NCF, a substrate of β-lactamase localized within the periplasmic space, is normally excluded from *E. coli* by the outer LPS layer. ONPG can be cleaved by β-galactosidase localized within the cytoplasm, but it is blocked from cell entry by the IM since the strain lacks *lac* permease. The inner and outer membrane permeabilisation was monitored spectrophotometrically over a time period up to about 1 h at 420 nm and 500 nm, respectively, using a Safire Microplate Reader (Tecan, Germany). Wells with 5 μM PMX, which efficiently permeabilises the *E. coli* membrane (Schindler and Teuber 1975) and wells without peptide were used as positive and negative controls, respectively.

Propidium iodide influx

To quantify the membrane disturbance (and morphological changes) due to peptide interaction, PI influx and DNA intercalation were determined using fluorescence-activated cell sorting (FACS). As with MIC studies, bacteria were cultivated until mid log phase, diluted to a final cell number of 5×10^5 per ml and exposed to 10 μg/ml PI in LB. The final peptide concentration corresponded to the MIC. PI intercalation into DNA results in pronounced fluorescence. Following Wickens et al. (2000) flow cytometric analysis of *E. coli* DH5α and *B. subtilis* DSM347 was performed on a FACSCalibur flow cytometer (Becton–Dickinson, Germany) equipped with a 488 nm argon laser. All detectors were used with logarithmic amplification. The bacterial suspension was incubated at 37°C and at time points (0, 5, 10, 20, 30, 60, 90 min) at least 10,000 events were recorded for each sample, using the Cell Quest software (Becton–Dickinson, Germany) for data acquisition and FCS Express (De Novo Software, USA) for analysis.

Hemolytic activity

The propensity of peptides to induce hemoglobin release from RBCs was determined after incubating 2.5×10^8 cells per ml for 30 min at peptide final concentrations between 1 and 200 μM in buffer (10 mM Tris, 150 mM NaCl, pH 7.4) for 30 min. After centrifugation, the absorbance of the supernatant was measured at 540 nm (V-550 spectrometer; Jasco, Japan) (Dathe et al. 2004). Zero hemolysis (blank) and 100% hemolysis (control) were read with cell suspensions incubated in buffer and 0.5% NH_4OH, respectively.

Cytotoxicity

Cell viability was detected by the MTT-assay as of described previously (Mosmann 1983). A total of 2.5×10^4 HeLa cells in DMEM with 10% fetal calf serum per well were seeded in a 96-well plate and allowed to grow for 24 h. After medium removal, the cells were exposed to increasing peptide concentrations for 1 h at 37°C. After washing, adding 180 μl PBS and 20 μl of MTT solution (5 mg/ml MTT in PBS) per well, and incubation at 37°C for 4 h, the solution was replaced by 100 μl of dimethylsulfoxide in each well. Cell viability was quantified by measuring the OD at 550 nm using a Safire

microplate reader (Tecan, Germany). The OD_{550} determined with untreated cells represented 100% viability.

Results

Peptide design

To investigate the role played by the aromatic cluster of cyclic R-,W-rich peptides with respect to their antimicrobial activity and cell selectivity in detail, the two W residues in cyclo-RRRWFW (c-WFW) were substituted with F (c-FFF), F was replaced by W, (c-WWW) and R and W were alternately arranged (c-WRW) (Table 1). The size of the cycle was enhanced by introducing additional aromatic and charged residues whilst conserving the amphipathic balance. The size-reduced pentapeptide c-WFW5 is characterized by a conserved WFW-domain but reduced charge. While the W–F exchanges were performed to study the specific role of the W-side chain without influencing the aromatic cluster and the cyclic backbone with two regular β-turns (Appelt et al. 2008), ring size modification and alternating R and W residues were expected to influence the backbone structure and to disturb the aromatic cluster.

Structural characterization

Reversed phase retention times, t_R, as a measure of hydrophobicity and amphipathicity of the cyclic peptides, are summarized in Table 1. Replacement of W with F and alternating the positioning of R and W in the cyclic hexapeptides reduced their interaction with the hydrophobic phase, whereas enlargement of the cycles from 6 to 12 residues and the loss of one R in c-WFW5 enhanced t_R.

CD-spectroscopy and fluorescence measurements were performed in order to monitor structural changes resulting from peptide binding to lipid bilayers. NMR studies had shown that c-WFW adopts a structure with two regular β-turns in a membrane-mimicking environment. In such environments, the clustered aromatic side chains of c-WFW are located in the hydrophobic compartment whereas the polar backbone and the charged residues reside in the lipid head group region (Appelt et al. 2008). The CD-spectrum of c-WFW dissolved in buffer shows a negative band and a shoulder at about 202 and 220 nm, respectively (Fig. 1). Binding to negatively charged liposomes resulted in a negative CD peak at 225 nm. As the 220–230 nm region contributions of the peptide group and aromatic residues superimpose, the band shift is assumed to reflect a change in the positioning of the side chains with respect to

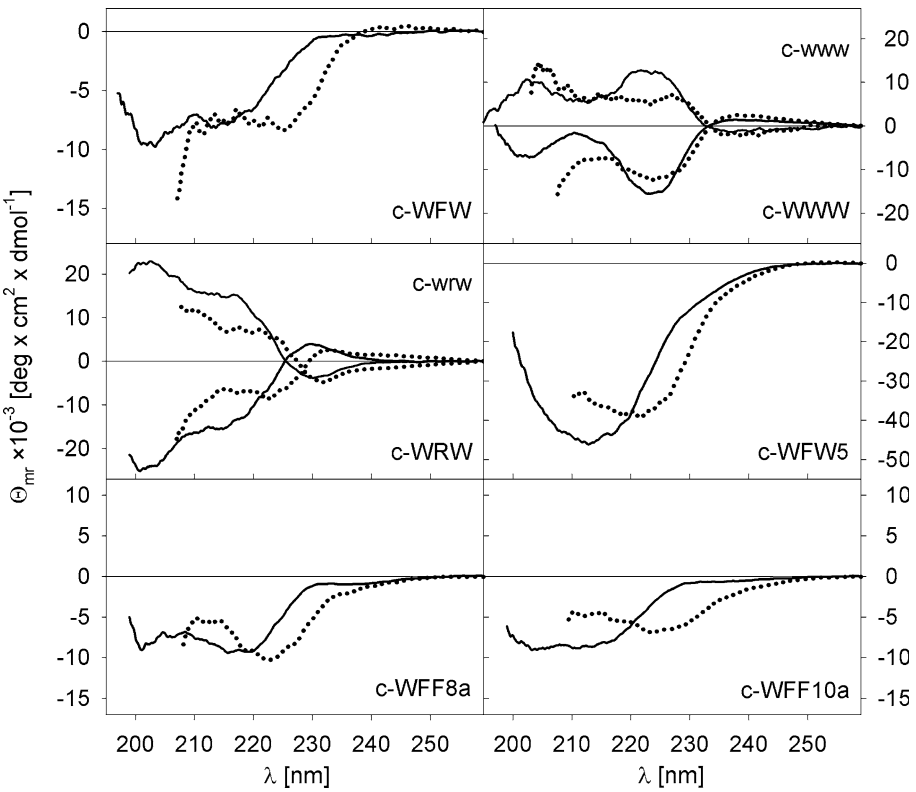

Fig. 1 CD-characteristics of cyclic peptides in the far UV in buffer (*solid line*) and in the presence of POPG SUVs (*dotted line*). The peptide concentration was 100 µM in buffer (10 mM Na_2HPO_4/NaH_2PO_4, 154 mM NaF, pH 7.4). The lipid concentration was 10 mM. $[\Theta]_{mr}$ is the mean residue ellipticity

the backbone and insertion of the hydrophobic cluster into the lipid acyl chain region. Conformational constraints seemed to increase with introduction of a third W residue (c-WWW) as reflected by less negative and strong negative peak intensity at 200 and 225 nm, respectively (Fig. 1). Evidence for the high stability of the WWW cluster was provided by the observed small CD changes at 225 nm after binding to POPG and the negligible influence of increased temperature, TFE and GuHCl in the near UV, where only the aromatic side chains contribute to the CD (compare Fig. 2a and b). Increase of temperature, the organic solvent and the denaturant are known to influence the chain flexibility and improve solubility of nonpolar groups, respectively. A reorientation of the aromatic residues in the presence of POPG is also suggested for c-RWR, indicated by the shift of the positive CD-band from 225 to 230 nm (Fig. 1). Large negative ellipticity values of c-WFW5 point to a more constrained structure compared to c-WFW (Fig. 1), whereas small spectral changes were observed with enlargement of the cycle to 10 (Fig. 1) or 12 residues. All-D amino acid sequences revealed mirror images.

A detailed structural interpretation of the spectra is difficult without other studies. However, comparable changes in the CD characteristics (ellipticity values and band position) of the POPG-bound peptides suggest that the amphipathic peptide structure, positioning and orientation of aromatic residues, should be comparable in lipid environment. Increase in the fluorescence intensity of W and the blue shift of the emission maximum from 253 nm in buffer to 341 nm when bound to liposomes suggest that c-WFW and c-WWW inserted into lipid bilayers much deeper than c-WRW which displayed a shift of only 6 nm (data not shown). In summary, the spectral changes reflect the membrane activity of the peptides. They may bind to and insert into lipid bilayers at different depths according to the t_R-pattern.

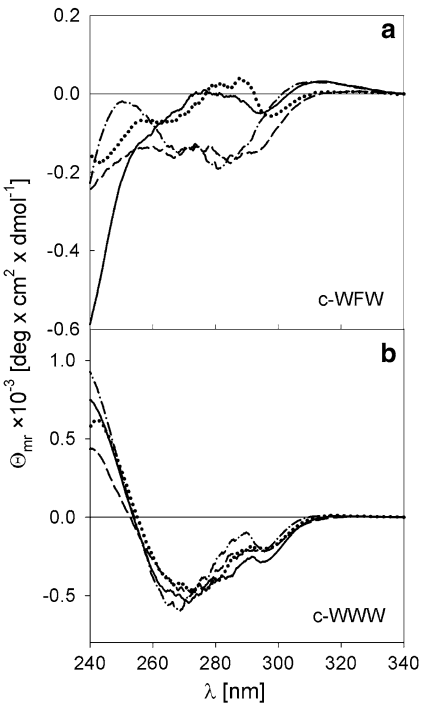

Fig. 2 CD-characteristics of c-WFW (**a**) and c-WWW (**b**) in the near UV in phosphate buffer at 20°C (*solid line*), 80°C (*dashed line*), in buffer/TFE 1/1 (v/v) mixtures (*dashed-dotted line*) and in the presence of 4 M GuHCl (*dotted line*). The peptide concentration was 100 μM in buffer (10 mM Na_2HPO_4/NaH_2PO_4, 154 mM NaF, pH 7.4)

Activity against bacteria and eukaryotic cells

The WFW aromatic residue motif of the cyclic hexapeptides displayed the highest antimicrobial activity and the lowest toxic effect against eukaryotic cells (Table 1). Three adjacent W residues (c-WWW) did not improve the antimicrobial effect and c-FFF and c-WRW were less active. Reduced cationic charge but conservation of the aromatic cluster in c-WFW5 slightly reduced the activity whereas increase in peptide size slightly improved the antimicrobial effect (Table 1). The activity changes were much more pronounced towards *E. coli*, although *B. subtilis* also showed similar patterns of increased susceptibilities. Undesired hemolytic activity and toxicity against eukaryotic cells counterbalanced the favorable antimicrobial properties of the large cyclic peptides. The activity profiles of the peptides largely correlated with the t_R-pattern as reported for other hexapeptide libraries with scrambled R-W-residues (Wessolowski et al. 2004) confirming that in addition to charge interactions, hydrophobic interactions with the cell envelopes are important for their antimicrobial effect. Furthermore, the identical activities observed for c-WWW and c-WRW and their corresponding all-D-amino acid cycles suggest that stereospecific interactions did not play a role. Based on all these experimental observations, the hexapeptide with the WFW motif represented the most active and *E. coli*-selective sequence.

Role of the *E. coli* outer membrane

A comparison of the activities of c-WFW against different *E. coli* strains and L-form bacteria reflects the important role of the outer membrane. Whereas the MICs of c-WFW were little changed between 5, 12.4 and 6.2 μM (DH5α, ML-35p, D21 strains, respectively) with strain variation, removal of the outer membrane (L-WF+) reduced peptide activity to 24 μM MIC (Table 1). Furthermore, studies with LPS-mutant strains (Fig. 3) demonstrated that the complete smooth LPS chemotype was required for maximal activity of c-WFW and c-WWW. Removal of the

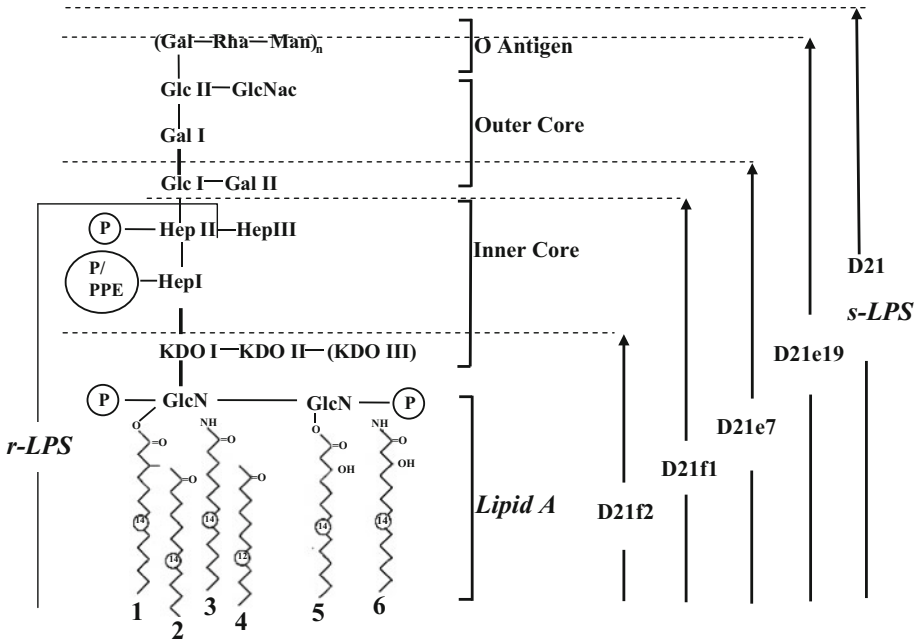

Fig. 3 LPS-mutant phenotypes. The mutants derived from the *E. coli* parent strain D21 are the following: D21e19 is deficient in carbohydrates close to the O-antigen region, D21e7 is galactose-deficient, D21ef1 is a glucose- and heptose-bound, phosphate-less LPS strain and D21f2 is a heptose-deficient LPS strain. The lipid A mutant strain MLK53 lacks the lauric acid residue. *Lipid A, r-LPS* and *s-LPS* schematically illustrate diphosphoryl lipid A from *E. coli* F583, the rough Rd-LPS from *E. coli* F583 and smooth LPS from *E. coli* K-235; respectively used in titration calorimetric binding studies

O-antigen and sugar residues of the outer core resulted in reduced activity (Fig. 4). These results are comparable with observations obtained with the same *E. coli* strains challenged with lactoferricin peptides (Farnaud et al. 2004). No activity changes however, were found for c-WRW and c-WFW5 (Fig. 4). With enlargement of the peptide cycle the activity profile towards LPS mutant strains (compare the MIC profile for c-WFW, c-WFW12) became comparable to the MIC pattern observed for the helical KLA1 (Fig. 4). The MIC continuously decreased with LPS truncation. The same activity pattern has been reported for other linear peptide sequences (Ramjeet et al. 2005).

The results suggest that interactions with LPS moieties are a prerequisite for maximal *E. coli* activity and selectivity of c-WFW. The structure of the cyclic R-,W-rich peptides and the cell specific lipid composition determine the activity profile of the peptides but seem also to modulate the mechanism of action. Both c-WFW and c-WWW not only inhibited the growth of *E. coli* but were bactericidal at the MIC. As demonstrated by the killing kinetics of *E. coli* strains D21 and D21f2 the number of CFUs drastically decreased or disappeared with time in the presence of c-WFW or c-WWW (Fig. 5). In contrast, the helical peptide KLA1 was not able to kill the bacteria at the MIC. After 120 min co-incubation, cell growth was comparable to that of the untreated control. These kinetics were observed with all the LPS mutant strains. The observations imply that the linear model peptide and the cyclic hexapeptides with the WFW or WWW motif possessed different mechanisms of action.

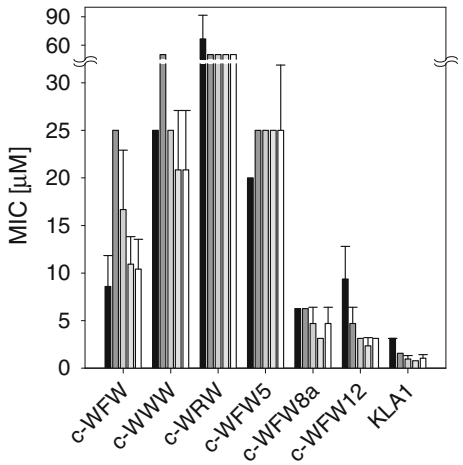

Fig. 4 Antibacterial activity of cyclic peptides and helical KLA1 towards LPS-carbohydrate mutant *E. coli* strains (Fig. 3). MIC is the minimal inhibitory concentration of bacterial growth for *E. coli* D21 (*black*) and the mutants D21e19 (*dark grey*), D21e7 (*grey*), D21f1 (*light grey*) and D21f2 (*white*). Presented is the mean MIC of three independent experiments performed in duplicate

Outer and inner membrane permeabilisation

Self-promoted uptake across the outer membrane (OM) caused by displacement of membrane-stabilizing cations (Hancock 1999) and permeabilisation of the inner target membrane have been suggested as the mode of action of the majority of antimicrobial peptides against Gram negative bacteria. c-WFW was able to permeabilise the OM of *E. coli*, but compared to PMX the activity was low (Fig. 6a). Below the MIC (12 μM) the peptide was not active against the OM and above the MIC, maximal

permeabilisation was reached within 10 min. The efficiency of the hexapeptides to promote transmembrane NCF transport correlated with the antimicrobial effect: c-WWW showed comparable activity, whereas c-WRW and c-FFF were much less efficient (data not shown). The activity of the most bactericidal c-WFW peptide against the inner *E. coli* membrane (IM) was very low (Fig. 6b). After 70 min there was no significant difference in ONPG uptake into the cytoplasm compared to untreated cells even at a peptide concentration of 54 and 162 μM. In contrast 5 μM PMX permeabilised the IM with high efficiency.

The low influx of propidium iodide (PI) into *E. coli* DH5α exposed to c-WFW at the MIC confirmed the low membrane permeabilising ability of the peptide (Fig. 7). In contrast, both PMX and the helical KLA1 model peptide were highly active in mediating PI uptake after only a short incubation time. Comparable activities of c-WFW and the model helical peptide were found with *B. subtilis* (data not shown).

These results suggest that peptide induced permeability of the outer membrane of *E. coli* modulated the transport and thus the accessibility of the peptides and other molecules at the inner membrane. However, the IM is likely not to be the sole (exclusive) target of cyclic hexapeptides like c-WFW and membrane permeabilisation seems not to be their preferred mode of action.

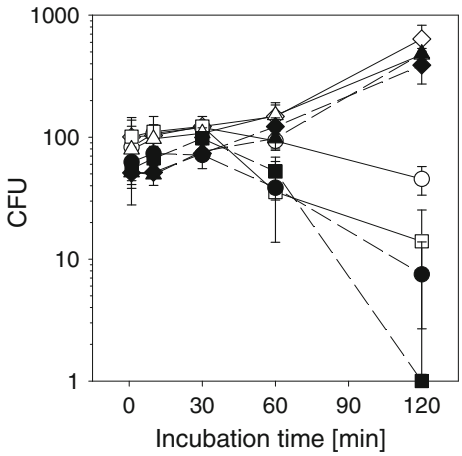

Fig. 5 Killing kinetics of c-WFW, c-WWW and KLA1 towards LPS-carbohydrate mutants. The number of colony forming units (CFUs) of D21 cells (*open symbols*) and D21f2 mutants (*black symbols*) co-incubated with c-WFW (*circles*) and c-WWW (*squares*) is shown in comparison to KLA1 (*triangles*) and the non-treated D21 as control (*diamonds*). The cells were exposed to the peptides at their corresponding MIC (Fig. 4). CFUs refer to plated 50 μl samples of 50-fold and 5000-fold dilutions of the peptide-treated and untreated cell cultures, respectively

Peptide interaction with lipid bilayers

Despite efficient binding to target bacterial membrane-mimicking vesicles, the permeabilising activity of the antimicrobial hexapeptides was very low. c-WFW induced only 20% dye release from negatively charged POPC/POPG LUVs at a peptide to lipid molar ratio of about 4/1 (100 μM peptide) (Fig. 8). Reduction and even elimination of the anionic bilayer charge enhanced the membrane disrupting activity even in the presence of bilayer-stabilizing cholesterol. c-WFW was not active towards POPE/POPG (3/1 mol/mol) bilayers up to a peptide to lipid ratio of 8.3/1. In contrast, at 100 μM KLA1 concentration dye release from POPE/POPG (3/1) LUVs was 35% and from

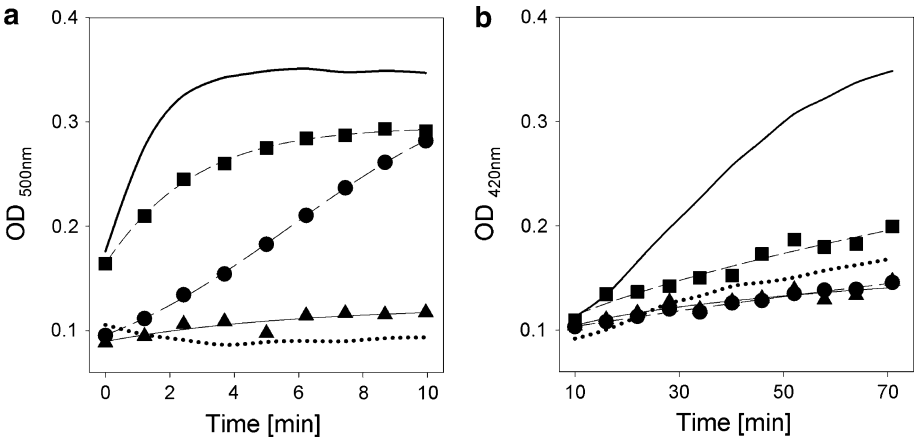

Fig. 6 Time-dependency of c-WFW-induced permeabilisation of the outer (**a**) and inner (**b**) membrane of *E. coli* ML-35p. The kinetics of peptide-mediated NCF passage across the outer membrane and ONPG passage across the inner membrane are monitored as change in the optical density (OD). The concentration of substrates was 20 μg/ml NCF and 100 μg/ml ONPG. The peptide concentrations were 6 μM (*triangles*), 12 μM (*circles*) and 54 μM (*squares*). OD-values for cells treated with 5 μM PMX (*solid line*) and untreated cells (*dotted line*) were measured as controls. Presented is one representative set of experiments (different peptide concentrations) performed two times in triplicate

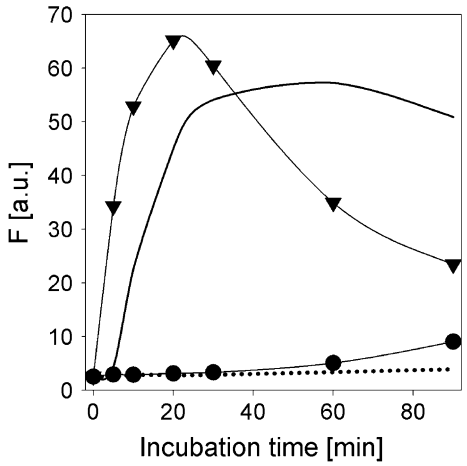

Fig. 7 Peptide-induced propidium iodide (PI) influx into *E. coli* DH5α. Presented is the FACS-derived mean fluorescence per cell (F) as result of PI (10 μg/ml) intercalation with DNA in the presence of c-WFW (*circles*) and KLA1 (*triangles*) at their MIC (4 and 6 μM, respectively). Cells permeabilised with 5 μM PMX (*solid line*) and untreated cells (*dotted line*) served as controls

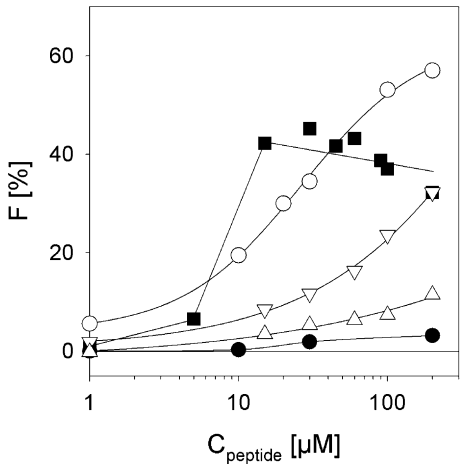

Fig. 8 Bilayer-permeabilising activity of c-WFW. Presented is the percentage of dequenching of the fluorescence (F) of calcein released from LUVs composed of POPC/cholesterol (3/1 mol/mol) (*open circles*), POPC/POPG (1/3) (*open triangles*), POPC/POPG (3/1) (*down open triangles*), POPE/POPG (1/3) (*black squares*), POPE/POPG (3/1) (*black circles*) after incubation with the peptide for 60 s. The lipid concentration was 24 μM in buffer (10 mM Tris, 154 mM NaCl, 0.1 mM EDTA, pH 7.4). At a concentration of 100 μM KLA1 dye release from POPE/POPG (3/1) LUVs was 35% and at 2 μM concentration the release from POPE/POPG (1/3) LUVs reached 100%

POPE/POPG (1/3) LUVs even 100% at 2 μM concentration (data not shown).

The increase of the fluorescence signal to about 40% observed for POPE/POPG (1/3 mol/mol) liposomes exposed to c-WFW and c-WWW at a 1/2 peptide to lipid ratio was related to a drastic increase in particle size as shown in Fig. 9. With a content of 75% negatively charged POPG of the liposomes (24 μM lipid concentration, about 9 μM accessible in the outer layer), aggregation at about 10 μM peptide concentration was related to a 1/1 molar ratio of peptide and POPG. Comparable c-WFW-caused vesicle aggregation was also observed for other negatively charged vesicles (Fig. 9). As shown in Fig. 10, each c-WFW injection into a POPE/POPG (3/1) suspension increased the turbidity caused by vesicles' aggregation. Absorption decreased under mechanical stress to the initial value and did not increase again with time (Fig. 10). Triton X-100 addition completely destroyed both aggregates and liposomes (Fig. 9). Fluorescence energy transfer studies confirmed that particle growth was not related to vesicle fusion (data not shown).

Taken together, vesicle charge dampening caused by peptide binding favored aggregation of intact liposomes and a net-cationic surface charge after disaggregation inhibited re-association. Comparable effects have been described for α/β antimicrobial peptides in interaction with PE-rich liposomes (Epand et al. 2005, 2006). Peptide binding promoted vesicle-vesicle contact, but the morphological changes did not result in leakage of the aqueous content from LUVs.

LPS binding

Isothermal titration calorimetric studies with lipid A-, r-LPS- and s-LPS-doped POPC liposomes (LPS moiety/POPC 12/1 mol/mol) (Fig. 3) demonstrated that interaction of c-WFW with the bilayers distinctly decreased with removal of the O-antigen and outer core oligosaccharides (Fig. 11). The Gibbs free energy of partitioning into lipid bilayers, ΔG° decreased in magnitude in the following order: POPC/s-LPS > POPC/r-LPS > POPC/lipid A. The hydrophobic partition coefficient, K_0 for POPC/s-LPS bilayers (1.9×10^4 M^{-1}) was almost one order of magnitude higher than that for lipid A-doped bilayers (4.2×10^3 M^{-1}). Lipid A and r-LPS differ with respect to their anionic charge whereas the outer core and O-antigen are free of charged groups. Based on our results, it appears that c-WFW is not binding to the cationic charges present in the inner core of LPS but instead it was interaction with the O-antigen and outer core polysaccharides which determined peptide partitioning and transport. The affinity of c-WFW for the LPS moieties was well correlated to the activity against corresponding LPS mutant *E. coli* strains (see Fig. 4).

Discussion

The CD-structural and affinity chromatographic studies demonstrate that the cyclic peptides containing the WXW

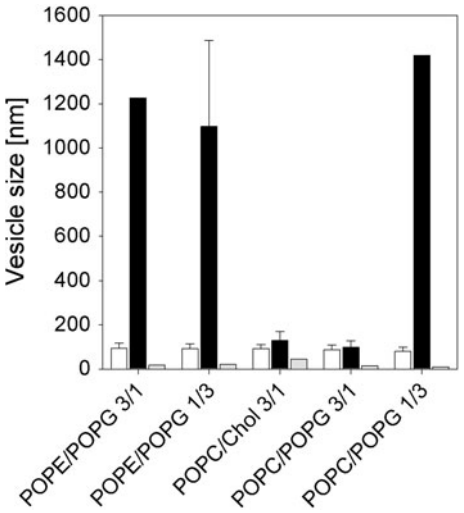

Fig. 9 c-WFW-induced changes in vesicle size. Presented is the size of LUVs of different lipid composition exposed to c-WFW (*black bars*) and after treatment with 0.4% Triton X-100 (*grey bars*) in comparison to peptide-free LUVs (*white bars*). The lipid concentration in buffer (10 mM Tris, 154 mM NaCl, 0.1 mM EDTA, pH 7.4) was 24 μM, peptide concentration was 100 μM (peptide to lipid molar ratio 4/1)

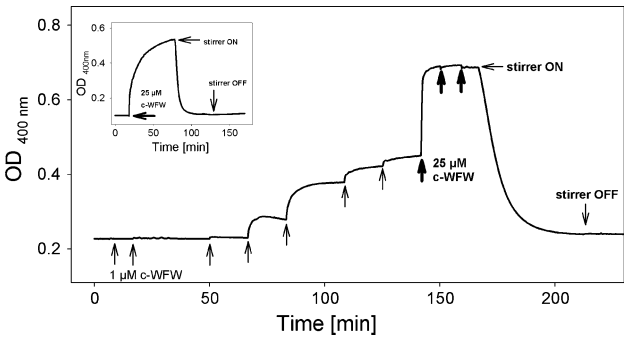

Fig. 10 c-WFW-induced turbidity of LUV suspensions. Presented is the increase in optical density (OD) of POPE/POPG (3/1 mol/mol) and POPE/POPG (1/3 mol/mol) (*insert*) suspensions after increase of c-WFW concentration in 1 μM steps (*thin arrow*) and 25 μM steps (*thick arrow*) without stirring. Mechanical stress (stirrer ON) resulted in OD-decrease. After switching the stirrer off again, no change in absorption was observed. The lipid concentration was 20 μM in buffer (10 mM Tris, 154 mM NaCl, 0.1 mM EDTA, pH 7.4)

motif (X = either W or F) are membrane active. As shown by NMR, the side chains of the aromatic residues point in the same direction when bound to micelles and the R residues are oriented to interact with the head groups of membrane mimicking systems (Appelt et al. 2008). These characteristics would be expected to facilitate interaction with the negatively charged lipopolysaccharides of the outer membrane of Gram negative bacteria and to promote insertion into the cytoplasmic membrane of most bacteria. Yet, despite efficient binding, the bilayer-disturbing activity of the cyclic c-WFW and c-WWW is low in comparison

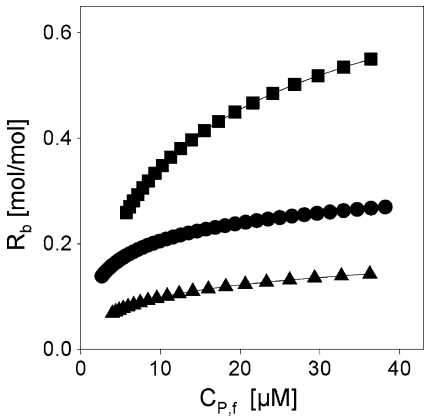

Fig. 11 ITC-derived binding isotherms of c-WFW for POPC/lipid A (12/1 mol/mol) (*triangles*), POPC/r-LPS (Rd mutant) (12/1 mol/mol) (*circles*), and POPC/s-LPS (12/1 mol/mol) (*squares*) SUVs. R_b denotes the molar ratio of bound peptide over accessible lipid, $C_{P,f}$ denotes the concentration of free peptide. Data were calculated by combining a surface partitioning equilibrium with the Gouy–Chapman theory (Keller et al. 2006)

to helical amphipathic peptides such as KLA1 (Dathe et al. 2002, 2004).

The low toxicity of the cyclic peptides towards eukaryotic cells can be explained by reduced accumulation at the electrically neutral lipid matrix, with any membrane disturbance or permeabilisation being driven by hydrophobic interactions according to the peptide amphipathicity. However, this explanation does not hold for the negatively charged bacterial target membranes. The *E. coli* inner membrane is composed of about 20% negatively charged lipids and 80% PE (Wilkinson 1988), whereas the membrane of *B. subtilis* is composed of negatively charged PG and cardiolipin and neutral PE at about 70/30% (O'Leary et al. 1988). The higher susceptibility of *B. subtilis* compared to *E. coli* to this type of cyclic R,W-rich hexapeptides has been associated in recent studies with differences in peptide accumulation at the membranes via electrostatic interactions (Junkes et al. 2008). However, the reduced barrier-disturbing activity towards negatively charged bilayers by the peptides, which has been reported before and has been associated with shallow partitioning into the membrane (Dathe et al. 2004), contrasts with their high antibacterial activity. This study shows that the most antimicrobial c-WFW was unable to permeabilise *E. coli*- and *B. subtilis*-modelling PE/PG-rich lipid bilayers even at an elevated peptide to lipid ratio of 8/1. Furthermore, we observed low permeabilisation of the inner *E. coli* membrane and little PI influx into *E. coli* and *B. subtilis* at the MIC. Thus, pore formation does not seem to be the dominating mode of action of cyclic hexapeptides with the WXW motif. This idea is supported by the observation that the MIC and bactericidal concentrations of c-WXW peptides are identical. In contrast, the membrane-permeabilising linear peptide KLA1

inhibits growth at the MIC but does not cause bacterial death.

Nevertheless, the activity of the cyclic peptides towards bacteria follows the amphipathicity (t_R) pattern, which makes sense, since interaction with the cell membrane is the first and most crucial step in their antimicrobial activity, irrespective of the specific details of the peptides' mode of action. With respect to cyclic hexapeptide membrane-activity, c-RRWWRF has been reported to induce demixing in DPPG/DPPE membranes (Arouri et al. 2009). Less intensive peptide-induced phase segregation of PG/PE mixtures was also observed with other peptides (Lohner et al. 2008) even with mixed α/β-amino acid sequences (Epand et al. 2006). The appearance of anionic lipid rich domains in PG/PE mixtures after peptide binding may have at least two consequences. Lipid demixing may interfere with certain regulatory functions of the cells (Matsumoto et al. 2006) either by influencing membrane protein functions or perturbing existing lipid domains in the membrane. Evidence for this latter mechanism comes from the detection of PE- or PG-enriched domains in the functioning plasma membranes of both *E. coli* and *B. subtilis* (Fishov and Woldringh 1999, Vanounou et al. 2003). Alternatively, the formation of lipid phase boundaries may result in packing defects through which polar compounds could translocate into the cytoplasm (Epand et al. 2008). Furthermore, the presence of PE-rich membrane domains can destabilize the bilayer because of the negative curvature tendency of the lipids (Epand et al. 2006). An alternative mode of action may involve peptides crossing the plasma membrane. Nicolas et al. reported that most of the peptides that are proposed to translocate across the cell membrane and attack internal cellular targets are rich in at least one or two amino acids such as tryptophan and arginine, histidine or proline (Nicolas 2009). With three arginine residues and at least two W, our cyclic hexapeptides fit into this category, and may therefore employ this mode of action.

With respect to anti-*E. coli* specificity, interaction with LPS in the outer membrane appears to modulate the peptide accessibility to the cytoplasmic membrane. This observation is supported by a correlation of the antimicrobial and OM-permeabilising activity of c-WFW analogs with substitutions of W by different non-natural residues (Bagheri et al. 2011). Recently, Epand et al. reported that the OM-permeabilising activity of a cationic sequence-random copolymer was progressively diminished with enhanced concentration while the effect upon the IM remained unaffected. The authors therefore suggested the existence of two peptide concentration-dependent mechanisms (Epand et al. 2008). Our c-WFW and c-WWW peptides very rapidly permeabilise the OM of *E. coli*. Thus, peptide transport across the OM is not rate-limiting for the accessibility at the inner membrane. Nevertheless, maximal activity of c-WFW and c-WWW does appear to be dependent upon interactions with the saccharides of the outer core and O-antigen of LPS. As both r-LPS and s-LPS have the same distribution of negatively charged phosphate groups, varied accumulation driven by electrostatic interactions does not provide an explanation for improved partitioning with extension of the carbohydrate chains in LPS mutant strains (Bagheri et al. 2011). Despite comparably high OM permeabilising activity, our cyclic peptides are expected to act differently from PMX, the high OM-perturbing activity of which is related to rapid competitive displacement of divalent cations from their negatively charged binding sites followed by insertion into the hydrophobic fatty acid chain region of LPS (Thomas et al. 1999). It may be that favorable contributions of the sugar moieties to peptide binding have to be considered, possibly related to peptides' cyclic structure. Carbohydrates are known to interact with peptides and proteins via stacking involving aromatic side chains (Laughrey et al. 2008), however the possession of an aromatic cluster alone may not fully explain the apparent LPS binding properties of our peptides. This may be further facilitated by the peptide structure, since it has been observed that the cyclic β-sheet AMP tachyplesin I showed a notably higher affinity for LPS than for acidic phospholipids, whereas its linear analogue and a helical magainin peptide cannot discriminate between the two (Hirakura et al. 2002).

In summary, c-WFW fulfills the structural prerequisites for membrane activity: cationic charge and amphipathicity. However, negative bilayer charge and PE lipids with an intrinsic negative-curvature tendency reduce the bilayer permeabilising effect of the peptide. The low permeability of the *E. coli* inner membrane and *B. subtilis* plasma membrane support the hypothesis that membrane permeabilisation is neither the only nor the dominating mode of action of the small cyclic R-W-rich peptide. Adjacent cationic and hydrophobic residues and a ring size of six amino acids caused maximal activity and selectivity towards bacteria. Specific interaction with LPS of the outer membrane modulates the transport to the IM, and hence the antimicrobial activity. Changes in amino acid positioning, ring size and modification of the lipid composition of the cell membrane lead to variations in the mode of action.

Acknowledgments We are very grateful to Heike Nikolenko (FMP) and Damian Rivett (King's College London) for the support in biological experiments. Sandro Keller (University of Kaiserslautern) is thanked for his contributions to the ITC studies. Jürgen Streich (IZW) is thanked for his support in the statistical analysis of MIC data. Martin Schulze (IFN, Schoenow/Bernau), Katrin Müller, Stephanie Speck (both IZW, Berlin) are thanked for their cooperation in the joint project on antimicrobial peptides. Finally, we are particularly thankful to Sebastian Farnaud (University of Westminster) and James Mason (King's College London) for their high interest in the work and their efforts to continue our fruitful cooperation. The work was

supported by the BMWi grant KF0376991MD6 and a DAAD scholarship (Ch. Junkes).

References

Appelt C et al (2005) Structure of the antimicrobial, cationic hexapeptide cyclo(RRWWRF) and its analogues in solution and bound to detergent micelles. ChemBioChem 6(9): 1654–1662

Appelt C et al (2008) Structures of cyclic, antimicrobial peptides in a membrane-mimicking environment define requirements for activity. J Pept Sci 14(4):524–527

Arouri A et al (2009) Peptide induced demixing in PG/PE lipid mixtures: a mechanism for the specificity of antimicrobial peptides towards bacterial membranes? Biochim Biophys Acta 1788(3):650–659

Bagheri M et al (2011) Interaction of W-substituted analogs of cyclo-RRRWFW with bacterial lipopolysaccharides: the role of the aromatic cluster in antimicrobial activity. Antimcirob Agents Chemother 55(2):788–797

Chan WC, White PD (2000) Fmoc solid phase peptide synthesis—a practical approach. Oxford University Press, Oxford

Chan DI et al (2006) Tryptophan- and arginine-rich antimicrobial peptides: structures and mechanisms of action. Biochim Biophys Acta 1758:1184–1202

Dathe M et al (1996) Peptide helicity and membrane surface charge modulate the balance of electrostatic and hydrophobic interactions with lipid bilayers and biological membranes. Biochemistry 35(38):12612–12622

Dathe M et al (2002) General aspects of peptide selectivity towards lipid bilayers and cell membranes studied by variation of the structural parameters of amphipathic helical model peptides. Biochim Biophys Acta 1558(2):171–186

Dathe M et al (2004) Cyclization increases the antimicrobial activity and selectivity of arginine- and tryptophan-containing hexapeptides. Biochemistry 43(28):9140–9150

Deres K et al (1989) In vivo priming of virus-specific cytotoxic T lymphocytes with synthetic lipopeptide vaccine. Nature 342(6249):561–564

Epand RF et al (2005) Bacterial species selective toxicity of two isomeric alpha/beta-peptides: role of membrane lipids. Mol Membr Biol 22(6):457–469

Epand RF et al (2006) Role of membrane lipids in the mechanism of bacterial species selective toxicity by two alpha/beta-antimicrobial peptides. Biochim Biophys Acta 1758(9): 1343–1350

Epand RF et al (2008) Dual mechanism of bacterial lethality for a cationic sequence-random copolymer that mimics host-defense antimicrobial peptides. J Mol Biol 379(1):38–50

Eriksson-Grennberg KG et al (1971) Resistance of *Escherichia coli* to Penicillins. J Bacteriol 108(3):1210–1223

Farnaud S et al (2004) Interactions of lactoferricin-derived peptides with LPS and antimicrobial activity. FEMS Microbiol Lett 233(2):193–199

Fishov I, Woldringh CL (1999) Visualization of membrane domains in *Escherichia coli*. Mol Microbiol 32(6):1166–1172

Friedrich CL et al (2000) Antibacterial action of structurally diverse cationic peptides on gram-positive bacteria. Antimicrob Agents Chemother 44(8):2086–2092

Hancock REW (1999) Host defense (cationic) peptides—what is their future clinical potential? Drugs 57(4):469–473

Hancock RE, Sahl HG (2006) Antimicrobial and host-defense peptides as new anti-infective therapeutic strategies. Nat Biotechnol 24(12):1551–1557

Hilpert K et al (2005) High-throughput generation of small antibacterial peptides with improved activity. Nat Biotechnol 23(8):1008–1012

Hirakura Y et al (2002) Specific interactions of the antimicrobial peptide cyclic beta-sheet tachyplesin I with lipopolysaccharides. Biochim Biophys Acta 1562(1–2):32–36

Junkes C et al (2008) The interaction of arginine- and tryptophan-rich cyclic hexapeptides with *Escherichia coli* membranes. J Pept Sci 14(4):535–543

Keller S et al (2006) Monitoring lipid membrane translocation of sodium dodecyl sulfate by isothermal titration calorimetry. J Am Chem Soc 128(4):1279–1286

Laughrey ZR et al (2008) Carbohydrate-pi interactions: what are they worth? J Am Chem Soc 130(44):14625–14633

Lehrer RI et al (1988) Concurrent assessment of inner and outer membrane permeabilization and bacteriolysis in *E. coli* by multiple-wavelength spectrophotometry. J Immunol Methods 108(12):153–158

Lohner K et al (2008) Liposome-based biomembrane mimetic system: implications for lipid-peptide interaction. Adv Planar Lipid Bilayers Liposomes 6:103–137

Matsumoto K et al (2006) Lipid domains in bacterial membranes. Mol Microbiol 61(5):1110–1117

Mosmann T (1983) J Immunol Methods 65:130–134

Nicolas P (2009) Multifunctional host defense peptides: intracellular-targeting antimicrobial peptides. FEBS J 276(22):6483–6496

O′Leary WM et al (1988) Gram-positive bacteria. In: Ratledge C, Wilkinson SG (eds) Microbial lipids. Academic Press, London, pp 117–201

Park KH et al (2008) Bacterial selectivity and plausible mode of antibacterial action of designed Pro-rich short model antimicrobial peptides. J Pept Sci 14(7):876–882

Pearson DA et al (1989) Trialkylsilanes as scavengers for the trifluoroacetic acid deblocking of protecting groups in peptide synthesis. Tetrahedron Lett 30:2739–2742

Ramjeet M et al (2005) Truncation of the lipopolysaccharide outer core affects susceptibility to antimicrobial peptides and virulence of *Actinobacillus pleuropneumoniae* serotype 1. J Biol Chem 280(47):39104–39114

Schindler PRG, Teuber M (1975) Action of Polymyxin-B on bacterial membranes—morphological changes in cytoplasm and in outer membrane of *Salmonella typhimurium* and *Escherichia coli*-B. Antimicrob Agents Chemother 8(1):95–104

Schnorrenberg G, Gerhardt H (1989) Fully automatic simultaneous multiple peptide synthesis in micromolar scale—rapid synthesis of series of peptides for screening in biological assays. Tetrahedron 45:7759–7764

Schuhmann E, Taubeneck U (1969) Sabile L-formen verschiedener *Escherichia coli*-Stämme. Zeitschrift Allg Mikrobiol 9:297–313

Seelig J (1997) Titration calorimetry of lipid-peptide interactions. Biochim Biophys Acta 1331(1):103–116

Thomas CJ et al (1999) Surface plasmon resonance studies resolve the enigmatic endotoxin neutralizing activity of polymyxin B. J Biol Chem 274(42):29624–29627

Vanounou S et al (2003) Phosphatidylethanolamine and phosphatidylglycerol are segregated into different domains in bacterial membrane. A study with pyrene-labelled phospholipids. Mol Microbiol 49(4):1067–1079

Wessolowski A et al (2004) Antimicrobial activity of arginine- and tryptophan-rich hexapeptides: the effects of aromatic clusters, D-amino acid substitution and cyclization. J Pept Res 64(4):159–169

Wickens HJ et al (2000) Flow cytometric investigation of filamentation, membrane patency, and membrane potential in *Escherichia coli* following ciprofloxacin exposure. Antimicrob Agents Chemother 44(3):682–687

Wiegand I et al (2008) Agar and broth dilution methods to determine the minimal inhibitory concentration (MIC) of antimicrobial substances. Nat Protoc 3(2):163–175

Wilkinson SG (1988) Gram negative bacteria. In: Ratledge C, Wilkinson SG (eds) Microbial lipids. Academic Press, London, pp 299–488